

Initiation of Femtosecond Laser Machined Ripples in Steel Observed by Scanning Helium Ion Microscopy (SHIM)

Bert Huis in 't Veld^{*1,2} and Hans van der Veer^{*2}

^{*1} *University of Twente, Faculty of Engineering Technology, Applied Laser Technology, Drienerlolaan 5, Enschede, Post Office Box 217, 7500 AE Enschede, The Netherlands*

E-mail: a.j.huisintveld@utwente.nl

^{*2} *TNO Science and Industry, Department Materials Technology, De Rondom 1, Eindhoven, Post Office Box 6235, 5600 HE Eindhoven, The Netherlands*

The physics of ablation has been studied experimentally with ultrashort laser pulses of 210 fs with a wavelength of 800 nm. A specimen of highly alloyed steel (alloy 800H) has been used. After the laser ablation experiments the surface has been inspected using SEM, AFM and scanning helium ion microscopy (SHIM). At the lowest fluence spherical bubbles are observed consisting of a mixture of gas and liquid having diameters in the range 20–90 nm. With increasing fluence the chain of events that has been observed consists of bubble forming and initiation of pre-ripples followed by a transformation towards regular coarse ripples with an orientation perpendicular to laser polarization direction. The pre-ripples have a different orientation that is not understood yet.

Keywords: initiation, bubbles, ripples, pre-ripples, femtosecond, ultrashort laser pulses, helium microscopy, laser ablation

1. Introduction

Ripple forming on surfaces of metals and other materials is widely observed, starting already a few years after the invention of lasers in 1960. Although the physics of ripple forming are studied worldwide, the initiation and growth mechanism still contain unanswered questions.

The study presented here is a continuation of a previous study [1] where pre ripples were reported and AFM images were presented. These pre ripples have spacings or wavelengths in the range 100 – 200 nm and an amplitude of about 10 nm. The orientation of pre ripples is far from perpendicular to the polarization direction of the laser light. It was observed that pre ripples transform into regular ripples with an orientation perpendicular to the polarization direction of the laser beam applied. The initiation started on small carbides present in the microstructure of the alloy used.

The wavelength of regular ripples depends on the fluence. Applying a laser spot with a Gaussian energy distribution for making a laser track on a metal surface, the largest wavelengths are found in the centre (typically 400 nm) whereas the edges of a track contain ripples with smaller wavelengths (typically 250 nm).

Models for explaining the initiation and growth of ripples can be divided into interference models [2] and models where self organizing is the main mechanism [3]. Pre ripples, varying ripple wavelengths and machine speed dependence are not consistent with the model of an interference modulated energy input transforming directly into the observed surface modulation. The model of self organizing structure formation can explain varying spacings, however the origin of pre ripples and the transition towards regular ripples are not explained.

To improve the understanding of ripple forming new experiments have been done on alloy 800H, an iron based

alloy with 30% nickel and 20% chromium. Low laser fluence levels have been applied to generate pre ripples in this alloy. Although this alloy contains high levels of nickel and chromium, much higher than the most common austenitic stainless steel, we have experienced that the interaction with short laser pulses of these iron based steel is similar.

To study the details of surface textures with pre ripples a relatively new method has been used for surface analysis: Scanning Helium Ion Microscopy (SHIM). With this technique the initiation of pre ripples and transformation towards regular ripples have been observed as present on the specimen surface after laser machining.

1.1 fs laser system

A titanium sapphire based laser system with a central wavelength of 800 nm was used for generation of the laser pulses. A seed/oscillator combination (Coherent Vitesse Duo) together with a regenerative amplifier (Coherent RegA9000) delivered pulses at 50 kHz repetition rate with 2 mW average power. The pulse length, measured by a second order auto correlator, was adjusted to 210 fs for all experiments. A combination of a rotary $\lambda/2$ wave plate and a beam splitting polarizing cube served as attenuator. The beam is horizontally polarized.

Manipulation of the bundle over the sample was accomplished by a two mirror galvo scanner system (Scanlab Scangine 14). A 100 mm f-theta lens (fused silica) focused the beam to an elliptical spot size with a long size of about 25 μm and a short size of about 17 μm . Due to the Gaussian energy distribution the effective spot size is smaller, here about 20 μm , see figure 5 .

The average fluence was determined by measuring the beam power at the exit of the scanner system with a power meter and dividing it by the repetition rate and the surface area of the laser spot. In all experiments the angle of inci-

dence of laser light was perpendicular to the specimen surface.

1.2 Specimen

Alloy 800 H is a highly alloyed (table 1) austenitic steel. The specimen used was cut from a piece of steel used for one year in industry at about 600 °C. Due to the industrial exposure to 600 °C small intergranular carbides have grown. In the previous study it was shown that the transformation of pre ripples towards regular ripples initiated on these small intergranular carbides. In order to remove these initiation sites we decided to dissolve these carbides by a solution treatment for 2 hours at 1100 °C with a water quench.

The specimen has been slightly etched before laser machining during 3 minutes with so-called V2A beize, an acid etchant with HCl and HNO₃. The microstructure of this alloy is depicted in figure 1 that shows the etched grain boundaries. Like many other austenitic steels this alloy contains twins, which are areas with straight boundaries and a structure that is mirror symmetrical from the surrounding grain.

Table 1 Chemical composition of X10NiCrAlTi 32 20 (alloy 800H)

Element	Fe	Ni	Cr	Ti	Al	Mn	Si	C
Wt %	bal	30-34	19-23	0.15-0.60	0.15-0.60	≤2.0	≤1.0	≤12

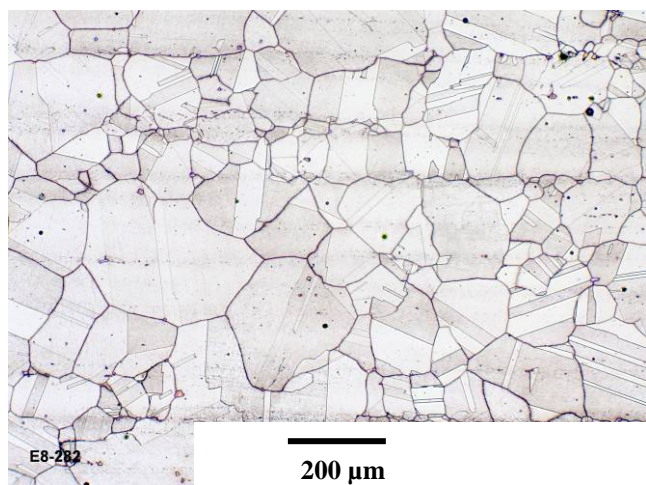


Fig. 1 Etched alloy 800H with a microstructure dominated by grain boundaries and twins (with straight boundaries)

1.3 Surface analysis

For surface analysis different techniques have been used: light microscopy, confocal light microscopy, scanning electron microscopy (SEM), atomic force microscopy (AFM) and scanning helium ion microscopy (SHIM) [4].

For an overview of well polished or etched surfaces light microscopy remains a powerful method. For better lateral resolution SEM is used with the advantage of a larger focus depth. For depth profiles and z-information in general, confocal light microscopy is used, however the lateral resolution of confocal light microscopy is limited. In this study pre ripples could not be imaged by confocal light

microscopy. With AFM it is possible to image pre ripples and to measure the amplitude of this surface modulation [1]. SHIM has been used to study the nanometer sized details of laser machined surfaces, since 30 keV helium ions generate secondary electrons in a very small image forming volume. Operation is basically analogous to a SEM except for using positive ions. The benefits of using helium ions for imaging are: ultrahigh resolution, different material contrast, good depth of focus and relatively low charging of insulators.

2. Experimental approach

Applying a fixed laser power of 2mW the scan speed and number of overscans are varied as depicted in figure 2. The scan speed is increased from left to right. Starting at 50 mm/s in the first column on the left to 100, 200, 400 and in the right column 800 mm/s.

The laser tracks in the first row are made by a single scan. In the second row one overscan is applied. The laser tracks in the third row are made with five scans and the tracks in row 4 with 10 scans. The lowest row contains lines made with 20 scans.

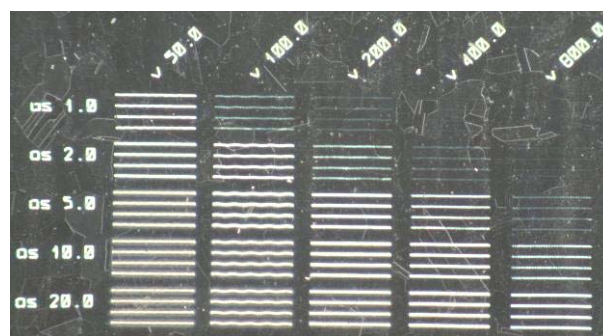


Fig. 2 Laser tracks on specimen surface. At each combination of scan speed and number of scans four identical lines are written. A single line is about 0.75 mm long.

For each combination of scan speed and number of scans four identical lines are written on the specimen. The lines written at 100 mm/s are not straight; a vertical vibration is superimposed to the horizontal lines. This vibration is caused by the dynamic behavior of the scanner.

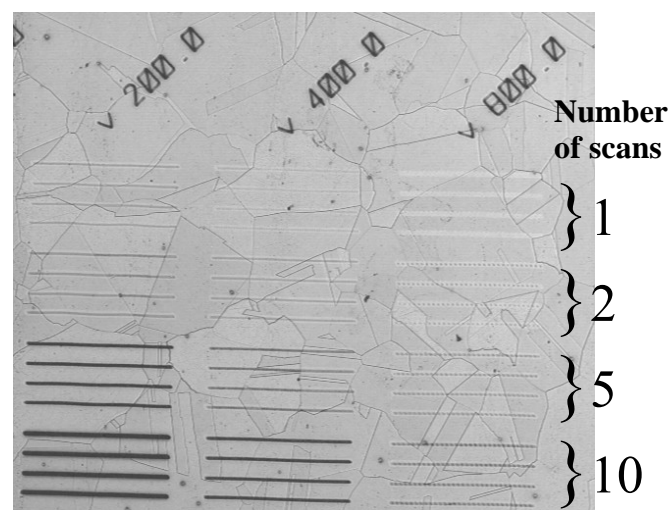


Fig. 3 Part of area depicted in Figure 2. Scan speed from left to right is 200, 400 and 800 mm/s. The number of scans is 1, 2, 5 and 10.

The four lines upper right in figure 2 are not visible. Therefore a second image is made, figure 3. In figure 3 upper right, the four lines made with a single scan and a speed of 800 mm/s are visible as light (white) lines. First impression is that the surface in the laser tracks has been cleaned. These lines have been analyzed further with SHIM.

Due to the etching procedure followed, the specimen contains steps with a typical step height of 100 nm. This is imaged in figure 4 where two laser tracks made in two scans and a scan speed of 100 mm/s are depicted.

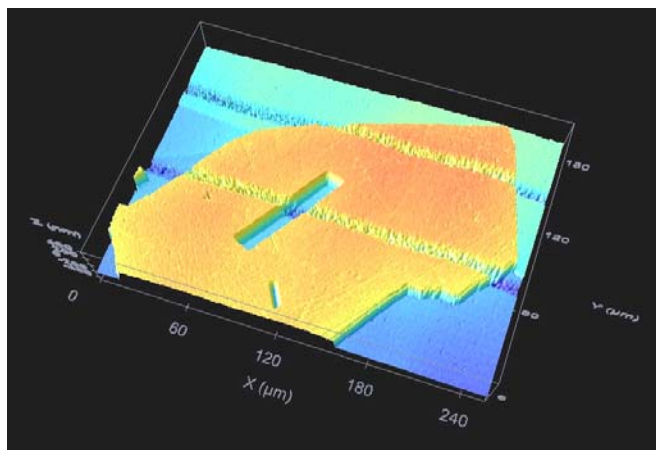


Fig.4 Confocal image of etched specimen surface containing steps. Two laser tracks are depicted. The length of the coloured area is 240 μm .

An average power of 2mW and a repetition rate of 50 kHz implies that each pulse contains 40 nJ energy. Assuming a circular spot size with diameter 20 μm an average energy intensity of 61 GW per cm^2 is calculated. Due to the Gaussian energy distribution the energy intensity in the central part of the laser spot will be about 122 GW per cm^2 .

3. Results

3.1 Lowest fluence

The lines produced with the lowest fluence (13 mJ/cm^2 on average) are the upper right ones in figures 2 and 3. Due to the velocity of 800 mm/s the laser beam shifts 16 μm between two pulses. As a result adjacent pulses show some overlap, but the central parts of the laser spot do not overlap. This is depicted in Figure 5.

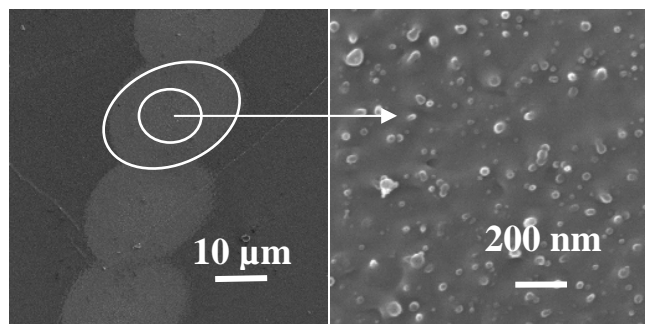


Fig.5 SHIM image of nano bubbles with diameters 20-50 nm in central part of an elliptical laser spot, the energy intensity was about 122 GW per cm^2 and small bubbles are formed.

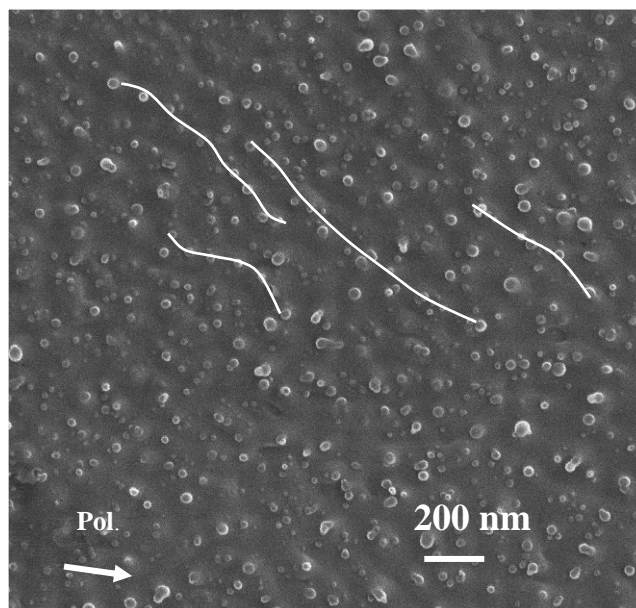


Fig. 6 Nano bubbles with diameters in the range 20–50 nm. The surface has a certain waviness as can be concluded from the contrast variations. Bubbles are preferentially found on surface ridges. In the upper half of the image four lines are drawn connecting bubbles on a ridge.

Nucleation of gas bubbles and development of a heterogeneous phase of liquid and gas is already described in 1998 [5]. Phase explosion as a decomposition of a thermodynamically metastable homogeneous liquid into a mixture of liquid droplets and gas follow from molecular dynamics simulations [6]. Images of initiation and growing nano sized bubbles have not been made before. That bubbles show a tendency to initiate on surface ridges is indicated by a few white lines drawn in figure 6.

3.2 Effect of a second scan

In the right column of figures 2 and 3 the second set of four lines is obtained by a second scan some 12 ms after the first one. After a second scan bubbles and pre ripples are found by SHIM in the central area of a laser pulse, figure 7. Bubbles are larger than those after the first scan in figures 5 and 6 and they are preferentially found on top of pre ripples. Obviously the ridges as found after the first scan (see figure 6) have been transformed into pre ripples.

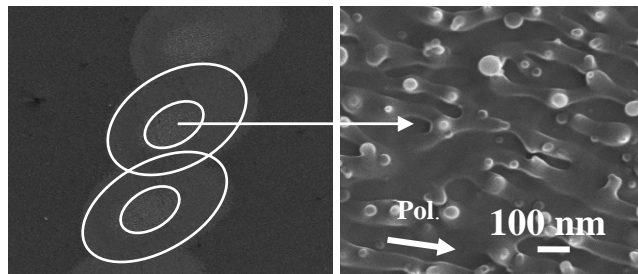


Fig.7 SHIM image of nano bubbles on pre ripples. Bubbles have diameters in the range 20 – 70 nm, some are necked. Pre ripples have wavelengths of about 122 nm.

These pre ripples have the same orientation as the surface ridges in figure 6 which is roughly the polarization direction of the laser beam as indicated in figure 7.

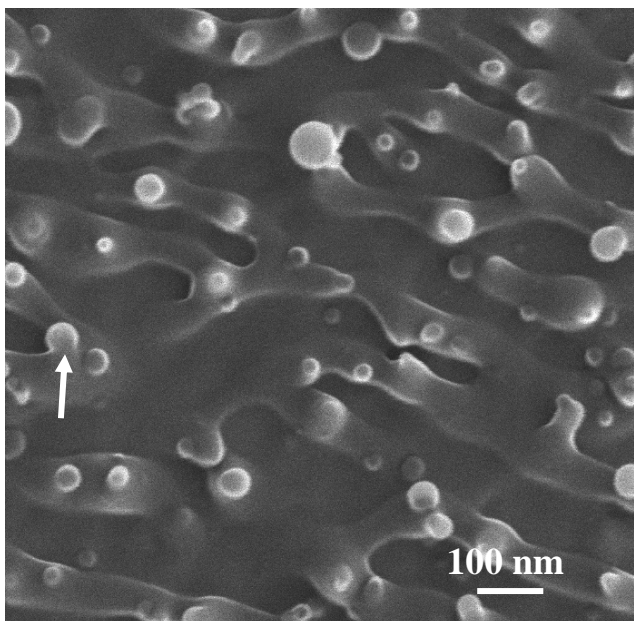


Fig. 8 Since the initiation of bubbles connected to pre ripples form the main result in this study, the image of fig 7 right, is printed a second time. Here the necking of one bubble (arrow) is well visible. By AFM the amplitude of pre ripples has been measured and a value of 32 nm (peak to valley) was measured.

3.3 Effect of multiple scans

With each scan more energy is pumped in the surface and also because the position of pulses in sequential scans is not exactly the same, the areas with pre ripples within a track are growing. After 5 scans within a track the individual laser spots still can be clearly recognized, after 10 scans the centre of the whole track is occupied with pre ripples and the first signs of regular ripples [7] appear, see figure 10.

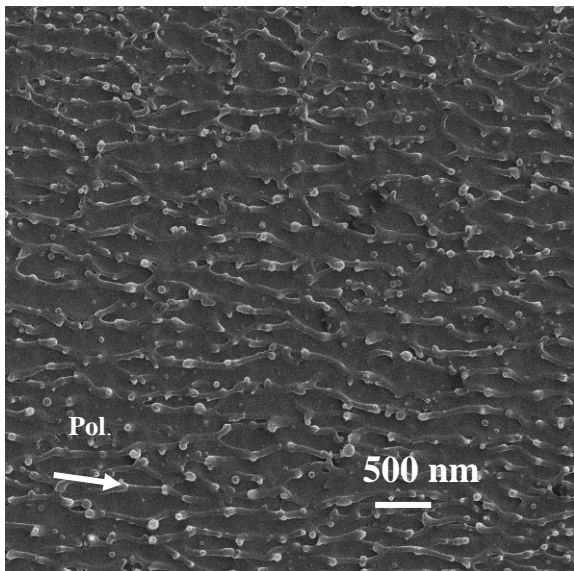


Fig. 9 SHIM image of a laser track after five scans (scan speed 800 mm/s). Area with bubbles and pre ripples. Almost all bubbles are connected to pre ripples; the wavelength of the pre ripples here is 172 nm. Regular ripples are not found.

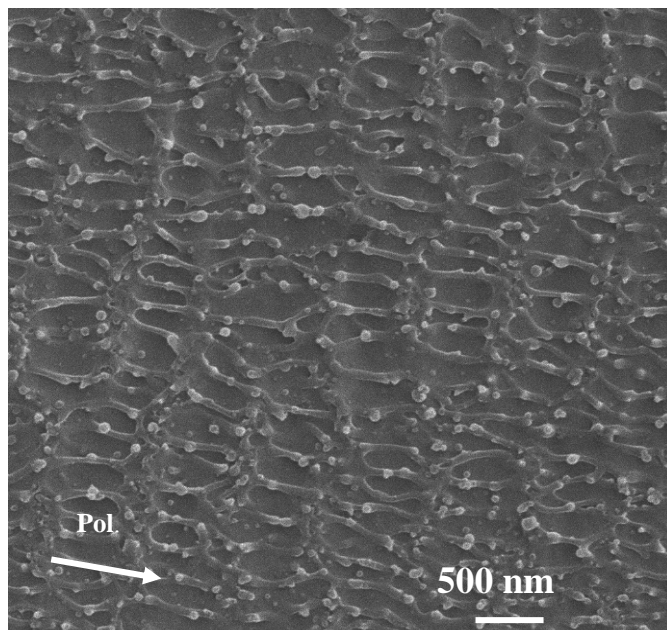


Fig. 10 SHIM image after 10 scans. Pre ripples have a wavelength of 192 nm. Besides bubbles and pre ripples also the orientation of regular ripples can be clearly recognized.

Regular ripples with an orientation perpendicular to the polarization direction (figure 10) form apparently grooves in the surface under pre ripples. Pre ripples bridge the course regular ripples and there is a strong interaction between bubbles and pre ripples as can be seen in figure 11.

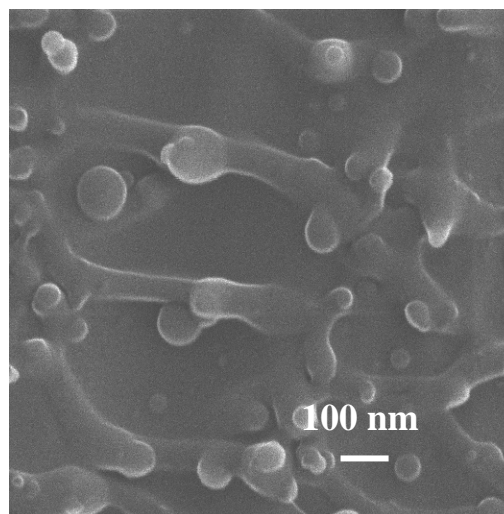


Fig. 11 SHIM image after 10 scans at 800 mm/s. Bubble has become a part of pre ripple. The diameter of the largest bubble is about 110 nm.

After 20 scans the regular ripples are the dominant surface feature. Pre ripples and bubbles can still be observed. As can be seen in figure 12, regular ripples are larger than pre ripples. The wavelength of the regular ripples in figure 12 is about 500 nm.

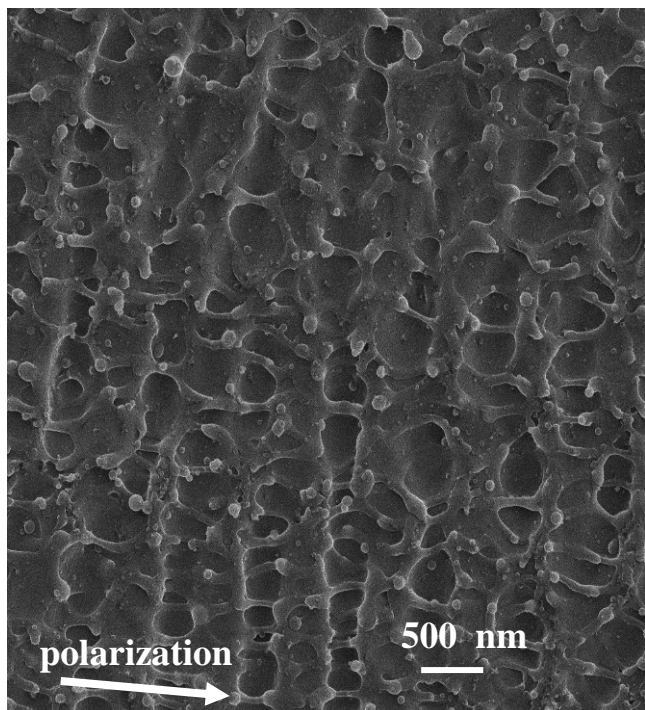


Fig. 12 SHIM image of regular ripples formed after 20 scans at the highest speed of 800 mm/s.

The surface features in figure 12 can be interpreted as a ductile response to tensile stresses. The origin of tensile stresses can be found in thermal expansion of the surface layer due to heating and superfast cooling under influence of laser energy. Both pre ripples and regular ripples have a fixed, but different orientation with respect to the polarization of the laser beam. However, the surface effects (bubble forming and ripple forming) can only start in the nanosecond regime and need the time between two pulses (20 μ s) to develop.

The polarization of the laser beam is only present at the surface during the pulse, which is during 210 fs. So the surface remembers the polarization of the laser light used (long) after the end of the laser pulse. So the question is raised: What is the memory mechanism active at the surface? [8] A mechanism where electrical charges are distributed in the surface under influence of polarization are a possible mechanism and are possibly a part of the answer, but this needs further analysis.

3.4 Influence of scan speed

Going back to the top row of lines in figure 2 we have laser tracks formed with different scan speeds and all other parameters identical. Starting with a scan speed of 50 mm/s figure 13, we have been working with strongly overlapping pulses. The pulse diameter is about 20 μ m and the laser beam shifts 1 μ m per pulse, so we generate 20 overlapping pulses. The results are imaged in figure 14. In figure 14a

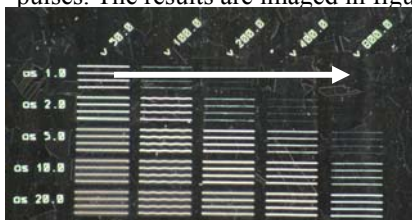


Fig.13 Lines made in one scan with increasing scan speed from left to right 50, 100, 200, 400 and 800 mm/s

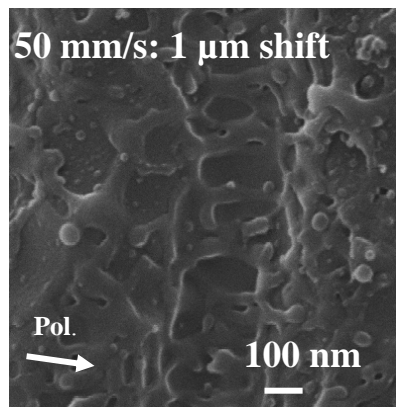


Fig. 14a

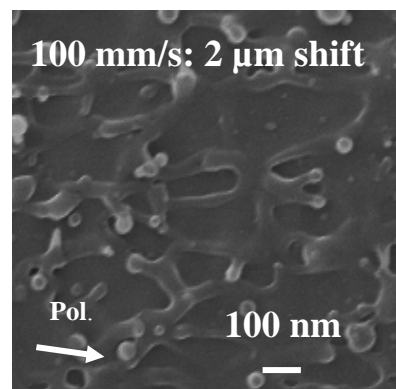


Fig. 14b

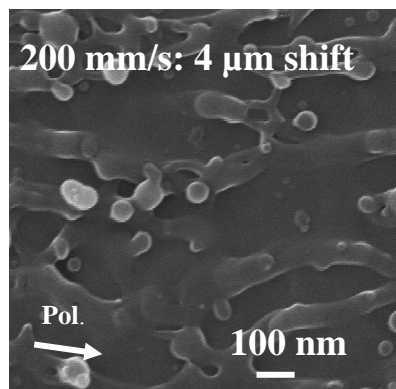


Fig. 14c

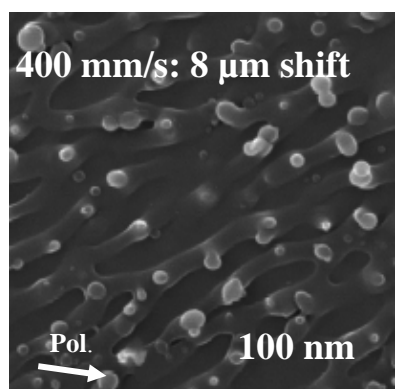


Fig. 14d

Fig.14 SHIM images after one scan. Increasing speed gives a larger shift between two pulses and reduces the overlap of sequential pulses. The degree of order increases from top to bottom.

The scan speed was 50 mm/s. In figure 14 b the scan speed was 100 mm/s resulting in about 10 overlapping pulses. In

figure 14c the scan speed was 200 mm/s resulting in 5 overlapping pulses. In figure 14d the scan speed was 400 mm/s resulting in a shift between two pulses of 8 μm , with a pulse diameter of 20 μm , the overlap is 2.5. Finally at the highest speed of 800 mm/s the pulses show almost no overlap as can be seen in figure 5 and we obtained only bubbles with a certain waviness in the surface. As indicated before the average fluence of a single pulse is 13 mJ/cm^2 and this value will be higher in the centre due to the Gaussian energy distribution.

We observe that in figure 14a at the lowest speed a regular ripple is visible, whereas in figure 14 d a pre ripple with bubbles is visible. With increasing speed the overlap and the fluence is lowered resulting in more regular surface features. Comparing figures 14d with figure 8 the influence of time between two pulses can be studied. In figure 8 the time between two pulses on same area is determined by the time between the first and second scan, which was a few ms. This is mainly waiting time before the second scan is started. In figure 14d the time is controlled by the repetition rate of 50 kHz and the time between two pulses is 20 μs .

The features in both figures are comparable. Both contain fine ripples connected with bubbles, although the width of ripples in figure 14c is a little smaller than in figure 8. From this observation we conclude that the time between two pulses has an influence on the texture that is developing due to the laser energy input. The longer time (ms) between two pulses causes a coarser ripple size. Because the relative position of pulses in two scans is not exactly known, the energy input can play a role as well.

3.5 Highest fluence

The highest fluence is obtained at the lowest scan speed (50 mm/s) and the highest number of scans (20), which are the conditions in the lower left corner in figure 2. The fluence there is about 4.1 J/cm^2 and the width of the laser track is 19 μm , see figure 15. In the centre of the track course regular ripples are observed, near the edges the regular ripples are finer. This has been observed before [1].

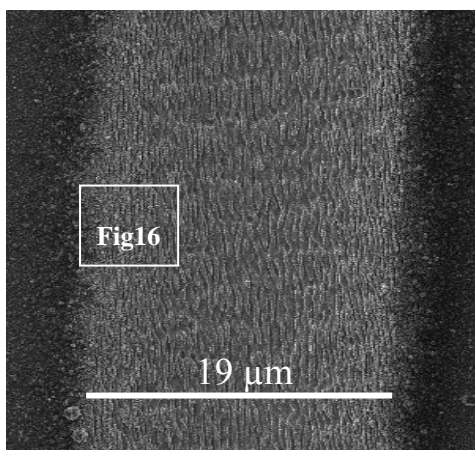


Fig.15 SHIM image of laser track made with 20 scans, 50 mm/s. Fluence = 0.5 J/cm^2 .

and is a reflectance of the Gaussian energy distribution over the width of a laser track. The edge of the laser track in figure 15 is imaged again in figure 16. The edges contain

some bubbles and large numbers of clustered particles. Outside the rippled area of 19 μm width a large amount of clustered particles is found. In this region bubbles escaping from the surface as well as coalescence of bubbles forming larger particles occurs.

In some images pre ripples can be observed in a stroke of about 1 μm width just outside the track with regular ripples.

Bubbles consist of frozen liquid containing gas, and have a perfect spherical shape (diameters 20 - 90 nm) due to the internal gas pressure. Clustered particles are larger, the largest in figure 16 are about 250 nm in diameter. Due to the higher fluence the surface temperature becomes higher and one can imagine that the facets of the particles are crystallographic planes which are formed during cooling in the ns- μs range.

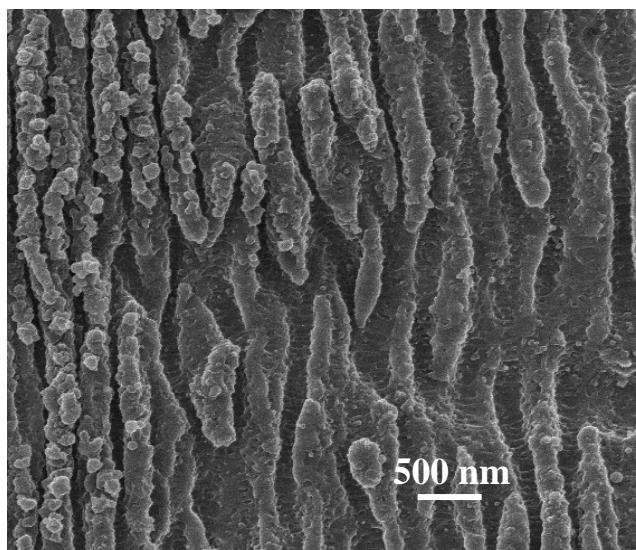


Fig.16 Edge of the laser track in fig.15. Coarse ripples with clustered particles. In the valleys of ripples the orientation of pre ripples is still visible.

It is observed that the valleys of regular ripples contain the remainders of pre ripples. Similar structures are observed for other materials: InP, Si, GaP [9]. So probably also in many other materials pre ripples and the transition towards regular ripples occurs at low fluence levels.

4. Sequence of events: bubbles, pre ripples and regular ripples

The (solidified) mixture of gas and liquid will probably have a high refractive index and it can play a role as a local field concentrator and initiator of surface plasma waves. The interaction between bubbles and surface ridges as depicted in figure 6, leads to pre ripples connected with bubbles, see figure 8. In bubbles the gas to liquid ratio will be higher than in pre ripples. The images suggest that pre ripples have more viscous properties.

In this study we have clearly seen that at low average fluence levels starting at 13 mJ/cm^2 bubbles are formed, whereas a double scan generates pre ripples interacting with bubbles.

Bubbles trying to escape from a pre ripple have been observed frequently. After 10 scans with the same fluence or 10 overlapping pulses regular ripples start to appear,

after 20 scans regular ripples and coalescence of bubbles become dominant. Of course the energy input in 10 scans is spread over a larger time span than a single scan with a 10-times lower scan speed. The time between two pulses in a single scan with repetition rate 50 kHz is 20 μ s whereas the time between two scans is in the ms range. And besides this factor 1000 difference in time, there is also the uncertainty of relative pulse positions in different scans. This uncertainty can cause a certain, but in general small variation in fluence along a laser track.

Multiple scans give the same sequence of features as overlapping pulses. Starting with a single (low energy) pulse only bubbles are obtained. This is the condition in the upper right corner in figures 2, 3 and 13. Going to more overscans or lower scan speed produces first fine ripples in strong interaction with bubbles. Only after 20 overscans or a factor 16 speed reduction, regular ripples become the dominant surface feature.

A scheme of the different morphological phenomena after irradiation of silicium is given in [10] showing separated fluence regimes for bubbles and ripples. Similar phenomena are observed in this study with steel (alloy 800H) as specimen material. The strong interaction of pre ripples with bubbles as depicted in figures 8-11, has not been observed before.

5. Discussion

The sequence of events with increasing fluence is bubbles that change towards a co-existence of bubbles with pre-ripples and finally regular ripples. A description of the electromagnetic interaction of a laser pulse with a metallic surface is required to start the process of understanding this sequence of events. Starting with a relatively flat surface bubbles are generated with a preference to align on surface ridges (figure 6) and we observe that the alignment of bubbles is a first sign of the orientation of pre ripples. When a second pulse arrives at the surface the bubbles are already solidified and obviously the interaction of subsequent laser pulses with aligned bubbles generates pre ripples. From the similarity in orientation and dimensions of bubbles on surface ridges and pre ripples we conclude that probably the same physical mechanism is active.

The nano sized laser induced periodically surface structures (LIPSS) are found after laser machining with the lowest fluence levels. Only by careful inspection of a surface the nano sized bubbles and pre ripples are found. Therefore we can imagine that in the past nano sized textures are missed. This idea is supported by careful inspection of figures with regular ripples elsewhere in literature e.g. [9]. So probably also in many other materials pre ripples and the transition towards regular ripples occur. Therefore lower fluence levels are an attractive process parameter to obtain self ordered nanostructures. Creation of a high degree of order with a large number of (very) low energy pulses is an attractive way to generate a higher degree of ordering. The potential of this approach is demonstrated in [11] where 40 nm wide grooves with an orientation perpendicular to the laser polarization direction are formed in synthetic single-crystal diamond surfaces by machining below the ablation threshold.

With increasing fluence pre ripples transform into regular ripples. The physical mechanism for this transition is unclear; however one may argue that with higher fluence also thermal effects will become stronger. The importance of thermal effects is supported by the observation that the time interval between the first and second pulse is not critical. A time interval of microseconds and of milliseconds cause more or less the same effects, compare figures 8 and 14d.

The physics behind the orientation of pre ripples and the transition towards regular ripples need further attention starting with a thorough description of the interactions of a single pulse with electrons and phonons in a metal.

6. Conclusions

1. At the lowest fluence, 13 mJ/cm^2 on average, with an energy intensity of about 122 GW per cm^2 , small bubbles with diameters 20-50 nm, are formed preferentially on surface ridges.

2. With increasing fluence aligned bubbles connected to pre ripples, wavelength 122 nm, with an orientation parallel to the polarization direction of the laser beam, transform into regular ripples with an orientation perpendicular to laser polarization.

3. Images of regular ripples in literature give reason to believe that pre ripples are formed in many materials at low fluence levels.

4. At the highest fluence 4.1 J/cm^2 clustered particles with diameters of about 250 nm are found presumably due to coalescence of bubbles.

Acknowledgments

- (1) BSIK NanoNed funding for Scanning Helium Ion Microscopy is acknowledged.
- (2) Support of TNO's KAVOT programme is acknowledged
- (3) fs laser experiments by Lightmotif, Ronald Sipkema, are acknowledged.

References

- [1] Bert Huis in 't Veld, Max Groenendijk, Hartmut Fischer, JLMN, 3, (2008) 206
- [2] J.E.Sipe, J.F.Young, J.S.Preston, H.W. van Driel, Physical Review B, 27, (1983), 1141
- [3] T.Aste, U.Valbusa, New Journal of Physics 7 (2005) 122
- [4] R.Hill, J.Notte, B.Ward, Physics Procedia (2008)135-141
- [5] K. Sokolowski-Tinten, J. Bialkowski, A. Cavalleri, D. von der Linde, A. Oparin, J. Meyer-ter-Vehn, S.I. Anisimov, Physical Review Letters, 81, (1998) 224
- [6] L.J. Lewis, D. Perez, Applied Surface Science, 2007.
- [7] J.Reif, F.Costache, M.Bestehorn, Recent advances in Laser Processing of Materials, 275-290, Elsevier 2006
- [8] Question raised by J.Reif at LAMP 2009, Kobe, Japan
- [9] A.Borowiec, H.K.Augen, Applied Physics Letters, 82, (2003) 4462
- [10] J.Bonse, S.Baudach, J.Krüger, W.Kautek, M.Lenzner, Applied Physics A 74, (2002), 19
- [11] M.Shinoda, R.R.Guttass, E.Mazur, J.Applied Physics, 105, 053102 (2009)

(Received: October 7, 2009, Accepted: December 25, 2009)